

Long-Range Wireless Interrogation of Passive Humidity Sensors Using Van-Atta Cross-Polarization Effect and Different Beam Scanning Techniques

Dominique Henry¹, Jimmy G. D. Hester², Hervé Aubert, *Senior Member, IEEE*,
Patrick Pons, and Manos M. Tentzeris, *Fellow, IEEE*

Abstract—This paper presents a method for the remote interrogation of batteryless humidity sensors based on statistical estimations and 3-D beam scanning techniques. As a proof-of-concept demonstration, a Van-Atta reflectarray sensor is interrogated with a 24-GHz frequency-modulated continuous-wave transceiver at various reading ranges. The extension of the proposed approach to passive or moving sensors is reported, and the measurement results are discussed. The relative humidity (RH) is derived from the statistical analysis of multidimensional radar echoes, while method is proposed to detect the sensor among clutter without knowing its exact position. Moreover, it is demonstrated that the cross-polarization effect of the Van-Atta reflectarray combined with the 3-D beam scanning technique allows the indoor measurement of the RH up to 58 m.

Index Terms—Antennas arrays, batteryless sensors, chipless sensors, direction-of-arrival (DoA) analysis, flexible electronics, Internet of Things, microstrip antenna arrays, radar imaging, radio-frequency identification (RFID) sensors, remote sensing.

I. INTRODUCTION

WITH the explosion of active electronic devices with integrated sensors, the remote reading of physical quantities is no more challenging in Internet of Things related applications. Nevertheless, the electromagnetic waves propagation, typically required for the wireless transmission of sensor data, imposes serious limitations in terms of the maximal range of interrogation, the multisensors interrogation capability, the embedded battery lifetime and the available frequency bandwidth. These constraints limit the applicability and the performance of wireless sensor network (WSN) technologies in numerous practical scenarios. WSN devices are often commercialized under different protocols of communication such

Manuscript received July 4, 2017; revised September 25, 2017; accepted October 20, 2017. Date of publication November 20, 2017; date of current version December 12, 2017. This work was supported in part by the French Technological Research Agency, in part by DTRA, in part by Ovalie-Innovation, in part by Occitanie Region under the CARANUC project, and in part by H2020-ICT under the DOSIRA-GATEONE project. This paper is an expanded version from the IEEE MTT-S International Microwave Symposium Conference, Honolulu, HI, USA, June 4–9, 2017. (*Corresponding author: Dominique Henry.*)

D. Henry, H. Aubert, and P. Pons are with LAAS-CNRS, 31031 Toulouse, France (e-mail: dhenry@laas.fr).

J. G. D. Hester and M. M. Tentzeris are with the School of Electrical and Computer Engineering, Georgia Institute of Technology, Atlanta, GA 30332 USA.

Color versions of one or more of the figures in this paper are available online at <http://ieeexplore.ieee.org>.

Digital Object Identifier 10.1109/TMTT.2017.2769055

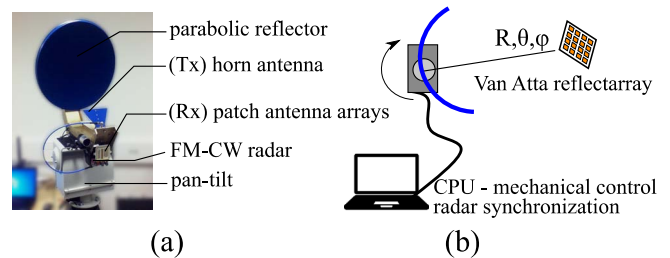


Fig. 1. (a) FMCW radar interrogation system. Tx and Rx antennas have orthogonal linear polarizations to take advantage of the cross-polarization effect of the relative humidity passive sensor. The mechanical beam scanning in azimuth and elevation is performed using a pan-tilt [4]. (b) Pan-tilt and radar system are synchronized to perform the beam scanning.

as Bluetooth low energy, ZigBee, or LoRa [1]. Typically, the end nodes of these networks are active devices with integrated circuits and batteries that generate specific frames for communication. The battery lifetime of such sensors can last up to 10 years for specific configurations and use cases. However, due to the active nature of the required circuitry, compounded by the mW power consumption levels of their transceivers during transmissions, such battery lifetimes can only be achieved at the cost of heavy duty cycling. Such operation is inappropriate for time-sensitive sensing and monitoring applications. Moreover, the wireless measurement of physical quantities becomes especially challenging in harsh environment that limits the amount of human intervention, such as very high or very low temperature and pressure, or even radioactivity. Hence, continuously interrogated sensors with long lifetime and long achievable range are highly required. One possible solution is the use of remotely readable passive sensors (without integrated devices and dc power supply) because their lifetime depends only on their constitutive material properties. However, the main technical challenge lies in deriving the physical quantity of interest from the measurement of sensors' electromagnetic echoes at a very long interrogation range.

Several technologies are currently used to perform effectively the remote interrogation of passive sensors. Radio-frequency identification (RFID) technology is widely utilized in many applications for both tag identification (based on a barcode reading) and tag sensing. However, power regulations

do not allow RFIDs to achieve a sufficient interrogation range (typically < 10 m) in applications where environments are harsh and highly reflective (note that surface acoustic wave sensor interrogation has been demonstrated in [2] for range up to 30 m in specific configurations). In addition, working at low frequencies can be problematic for the integration of small antennas. Moreover the electromagnetic to acoustic wave transitions can further degrade the range of interrogation. Other technologies at higher frequencies exist, such as passive millimeter-wave identification sensors working around 60 GHz, allowing the miniaturization of passive tags, like pressure sensors [3], and featuring a range of interrogation of only few meters.

This paper is originally based on a previous version which proposes for the first time an alternative technique to the standard RFID interrogation in order to locate and remotely read flexible passive humidity sensors at long interrogation ranges (> 50 m) [4]. The present extension reports the more detailed description of three different beam scanning techniques, including the synthetic aperture radar (SAR) beam scanning approach. Moreover, an enhanced estimation of the humidity is proposed here from adding additional contributions to the measured echo level distribution, and by improving the linearity of the long-range relative humidity (RH) estimation. Finally, it is shown that the RH at the sensor location can be derived from the proposed beam scanning techniques even if undesirable clutters are present inside the volume of analysis. The sensor tag can be used to monitor the humidity on targeted areas with difficult access, and avoids battery replacement in structural health monitoring applications. The obtained long-range interrogation enlightens all the potential of such passive tags and the proposed method of interrogation can be extended to the wireless measurement of various physical or chemical quantities using Van-Atta reflectarray sensors.

The proposed technique merges technologies from two different domains: 1) a frequency-modulated continuous-wave (FMCW) scanning method involving signal processing, SAR, and statistical estimators and 2) the design of passive sensors using humidity-sensitive Kapton-based Van-Atta retrodirective arrays. This original technique was already introduced in [5] and [6] although there was no report of its use for an integrated passive sensor and, at such a long distance and with the measurement sensitivity reported here. The sensitivity improvement is mainly due to the combination of the cross-polarization and retrodirective effects of the reflectarray which enhances the signal-to-noise-ratio (SNR). Moreover, this kind of humidity passive sensors was wirelessly interrogated at only 5.5 m [7] and detected at 30 m [8]. Such results require at least a 4-GHz frequency band (13%) around 30 GHz to perform the required full-scale dynamic range measurement.

The first part of this paper describes the hardware used for the interrogation technique as well as the properties of the Van-Atta reflect array. Three mechanical beam scanning techniques are described in detail here for the remote estimation of the RH with high accuracy: 1) the spherical beam sweeping performed by a stationary radar; 2) the cylindrical beam sweeping performed also by a stationary radar; and 3) the SAR obtained from the uniform linear motion of the

radar with constant velocity. The second part is focused on the indoor interrogation of the humidity passive sensors at different ranges of interrogation up to 58 m. Several methods are investigated in order to achieve the largest full-scale measurement range and the highest linearity. Special attention will be devoted to the definitions of statistical estimators from the Gaussian distribution of measured electromagnetic echoes and linearity corrections. A 3-D display of echoes using convenient isosurfaces is also reported with/without the presence of passive humidity sensors in a highly cluttered environment. Measurement results obtained from the remote reading of the Van-Atta reflectarray at different angles of incidence are finally discussed and a direction-of-arrival (DoA) analysis is applied to remove undesirable echoes.

II. WIRELESS INTERROGATION OF PASSIVE SENSORS

This section focuses on the hardware description of the reader (24-GHz FMCW radar mounted on a mechanical platform) and the passive humidity sensor (Van-Atta sensor reflectarray).

A. Radar Beam Scanning Description

The reader is often called short-range FMCW radar [9] because it allows targets detection below 100 m. However, it is actually a long-range reader when used for the wireless interrogation of passive sensors as it allows reading range above 5 m. More specifically it is demonstrated here that reading ranges of passive sensors up to 58 m are possible [4].

The 24-GHz FMCW radar from IMST GmbH (DK-sR-1030e model) transmits a so-called chirp that is a triangular frequency-modulated signal. In our proof-of-concept demonstration, the carrier frequency is of 23.8 GHz. This choice brings many advantages, such as: 1) a good achievable linearity of the radar voltage control oscillator over a wide frequency band ($B = 2$ GHz), which is mandatory for ensuring a sufficient depth resolution d ($d = c/2B = 7.5$ cm, where c denotes the velocity of light [10]); 2) an operating frequency in the ISM band; and 3) the design of small size passive sensors with integrated miniaturized antennas. The duration T of the up-ramp of the modulation is 5 ms and corresponds to a chirp rate B/T of 0.4 GHz·ms⁻¹. Note that the frequency band B used here exceeds the ISM band limits of 250 MHz. However, it has already been shown in [5] that it is possible to interrogate passive sensors in such narrower bandwidth, but at the expense of degradation in measurement sensitivity.

A mechanical beam scanning is performed as the transmitted (Tx) channel of the FMCW radar is connected to a rotating parabolic antenna with the gain of 33.5 dBi and the 3-dB beamwidth of 2° [see Fig. 1(a)]. The rotation has a step of 1° in azimuth and elevation. The mechanical pan-tilt (Pelco PT570P) is synchronized with the transmitted signal through a computer unit [see Fig. 1(b)]. The electromagnetic signals backscattered by the sensors are received (Rx) by two arrays of 1×5 patch antennas separated by the half-wavelength of the carrier frequency (6 mm). This separation distance allows deriving the DoAs of backscattered signals. The gain of the Rx-antenna is of 8.6 dBi and the beamwidths of this antenna

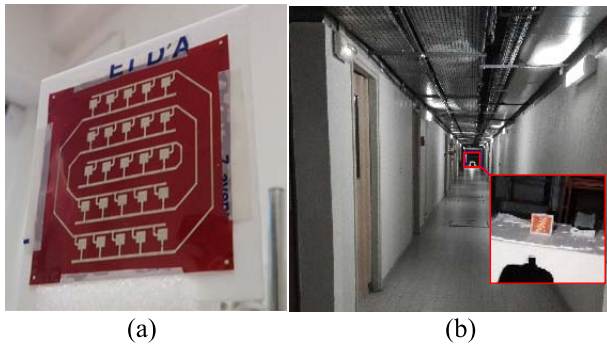


Fig. 2. (a) Kapton-based Van-Atta reflectarray prototype. (b) Long range (60 m) and indoor remote measurement setup of this prototype in a corridor [4].

are of 60° and 25° in azimuth and elevation, respectively. The Tx and Rx antennas are also positioned in orthogonal linear polarizations, in order to take advantage of the cross-polarizing properties of the printed Van-Atta humidity sensor. A spatial translation of the radar system is also performed. Let $df = 2D^2/\lambda$ be the Fraunhofer distance, where $D = 50$ cm is the largest antenna dimension of the parabolic dish diameter. Consequently, the theoretical separation distance between far and near-field regions stands at $df = 39.6$ m. The radar output power is 20 dBm (100 mW).

This platform is used here for comparing the performances of three possible mechanical beam scanning techniques for the remote interrogation of passive humidity sensors, that is: 1) the spherical beam sweeping; 2) cylindrical beam sweeping performed by a stationary radar; and 3) the SAR-type scanning obtained from the uniform linear motion of the radar with constant velocity.

The electronic beam scanning could be used instead of the proposed mechanical scanning. However, the mechanical beam scanning offers the advantage to perform accurate rotations both in azimuth and elevation, and contrary to the electronic scanning using fixed (static) antennas, it ensures the same beamwidth (i.e., the same angular resolution) in all beam directions, as Tx and Rx antennas keep unchanged their beamwidth during the rotation.

B. Kapton-Based Van-Atta Passive Humidity Sensors

The proof-of-concept passive humidity sensor used for the measurements is a 74×74 mm² Van-Atta reflectarray structure [see Fig. 2(a)]. It is composed of five side-by-side linear antenna arrays and inkjet-printed on an easily low-cost and integrable flexible substrate (Kapton HN polyimide). It has the property to retransmit the incident waves in phase and in cross-polarization. The linear antenna arrays of the tag are connected following the characteristic Van-Atta scheme. Contrary to basic Van-Atta reflectarrays, two connecting networks are here required in the structure, in order to connect both complementary polarization couples and thereby inducing a cross-polarization of the reemitted signal. As reported in [7] and [8], such flexible printed Van-Atta targets provide a simultaneously high and largely isotropic radar cross section that is, in addition, extremely robust to bending. These combined properties

confer high detectability from a large range of incident angles, as well as enable conformal mounting and polarimetric detection compatibility. Using the bistationary FMCW radar for the linearly polarized incident electromagnetic fields facilitates the detection of the passive sensor by increasing the SNR. Moreover the sensor ground plane allows the placement of the sensor in close proximity of metallic clutter without degrading its reradiating properties.

The permittivity of the Kapton is very sensitive to humidity of which a small change generates an observable shift of the device resonant frequency [8]. According to the substrate datasheet, the relative permittivity of the used Kapton is a function of RH as follows: $\epsilon_r = 3 + 0.008RH$.

Thus, an appropriately designed passive sensor at 24 GHz provides a measurable echo level fluctuation. To demonstrate the unique properties of the proposed reflectarray-based sensor wireless, indoor measurements of this sensor are performed in a long (60 m) corridor [Fig. 2(b)]. In comparison with outdoor or nonreflective environments, performing indoor measurement may generate significant multipath and decrease the SNR. This is generally due to high reflective cluttering objects, such as metallic grids or walls. It was intended to perform these measurements in such conditions to validate the experiment in a nonideal rugged environment.

III. MEASUREMENT RESULTS AND DISCUSSION

Different methods are detailed in this section to measure the RH from the wireless interrogation of Van-Atta reflectarray. In Section III-A, the structure of the multidimensional radar data grid for three mechanical beam scanning techniques (reported as solutions n^o1, n^o2, and n^o3) is described. The solution n^o1 (spherical sweeping) is then applied in Section III-B to interrogate the Van-Atta sensor reflectarray located at 1.3 m from the reader. Several estimators are derived to retrieve the RH. In Section III-C, solutions n^o1 and n^o2 are combined to perform the so-called *sweeping combination*. This beam scanning is applied for the wireless reading of a sensor reflectarray located at 10 m from the reader. In Section III-D, the solution n^o3 (SAR beam scanning) is reported. Measurement results for these different beam scanning techniques are reported in Table I. In Section III-E, the feasibility of interrogating Van-Atta sensor reflectarray at long ranges of interrogation (up to 58 m) is demonstrated.

A. Passive Sensor Remote Interrogation Using Three Different Multidimensional Radar Beam Scannings

The main principle of the multidimensional radar beam scanning (2-D or 3-D) is to analyze the signals backscattered by the passive sensor when using multiple directions of interrogation. Several beat frequency spectra (that is, one spectrum per direction of interrogation) are then obtained from the 3-D scanning, and processed in a volume of analysis composed of so-called voxels (When a 2-D scanning instead of a 3-D scanning is used, beat frequency spectra are processed on a surface of analysis composed of so-called pixels). To each voxel, a specific echo level is assigned and is expected to

TABLE I
ESTIMATORS PARAMETERS

Spherical beam sweeping performed by a stationary radar (solution n°1) Interrogation range : 1.3m				
estimator for RH [38%-69%]	D (dB)	η (dB/ %)	R^2	ε (%)
e_{Max}	13.7	-0.4	0.97	1.7
e_A	4.7	-0.1	0.98	2.0
e_S ($s=4$)	17.0	-0.6	0.97	1.5
e_S Corrected	17.0	-0.6	0.98	1.1

Sweeping combination (combination of solutions n°1 and n°2) – Interrogation range : 10.0m				
estimator for RH [34%-74%]	D (dB)	η (dB/ %)	R^2	ε (%)
$e_{Max} Opt - without clutter$	9.5	-0.2	0.97	2.5
e_S ($n=4, s=4$) – with clutter	10.5	-0.2	0.93	4.0
e_S ($n=3, s=4$) – with clutter	10.6	-0.2	0.93	4.0
e_S ($n=2, s=4$) – with clutter	10.0	-0.2	0.93	4.0
e_S ($n=1, s=4$) – with clutter	10.9	-0.2	0.92	4.5
e_S ($n=0, s=4$) – with clutter	10.3	-0.2	0.88	5.0

SAR-type scanning obtained from the uniform linear motion of the radar with constant velocity (solution n°3) – Interrogation range : 2.1m				
estimator for RH [20%-56%]	D (dB)	η (dB/ %)	R^2	ε (%)
$e_{Max} - PRI = 0.1$ s	9.0	-0.3	0.99	1.0
$e_{Max} - PRI = 1.0$ s	9.4	-0.2	0.98	2.0
$e_{Max} - PRI = 2.5$ s	10.5	-0.2	0.94	2.5
$e_{Max} - PRI = 3.0$ s	10.5	-0.2	0.86	6.0

D : dynamic range for the given RH range.
 η : sensitivity
 R^2 : linearity or coefficient of determination.
 ε : standard error or precision between the linear model and measurements

contain some information on the humidity at the passive sensor location.

Three mechanical beam scanings are considered here for the remote estimation of the RH: 1) the spherical beam sweeping performed by a stationary radar (solution n°1); 2) the cylindrical beam sweeping performed by a stationary radar (solution n°2); and 3) the SAR-type scanning obtained from the uniform linear motion of the radar with constant velocity (solution n°3). Each of these three scanings generates a specific voxel volume or surface which characterized the spatial resolution of the chosen scanning. The volume resolutions V_S (solution n°1) and V_C (solution n°2), and the surface resolution S_{SAR} (solution n°3) are given by

$$V_S = \left(2R^2d + \frac{d^3}{6} \right) \cdot \theta_S \cdot \sin\left(\frac{\phi_S}{2}\right) \quad (1)$$

$$V_C = R \cdot d \cdot d_x \cdot \phi_S \quad (2)$$

$$S_{SAR} = d \cdot v \cdot PRI \quad (3)$$

where R denotes the distance between the center of the voxel and the radar, while θ_S , ϕ_S , and d_x designate the steps in azimuth, elevation, and cross-range, respectively; d is the previously defined depth resolution (see Section II-A); v is the constant velocity of the radar during its uniform linear motion; PRI is the pulse repetition interval of the radar.

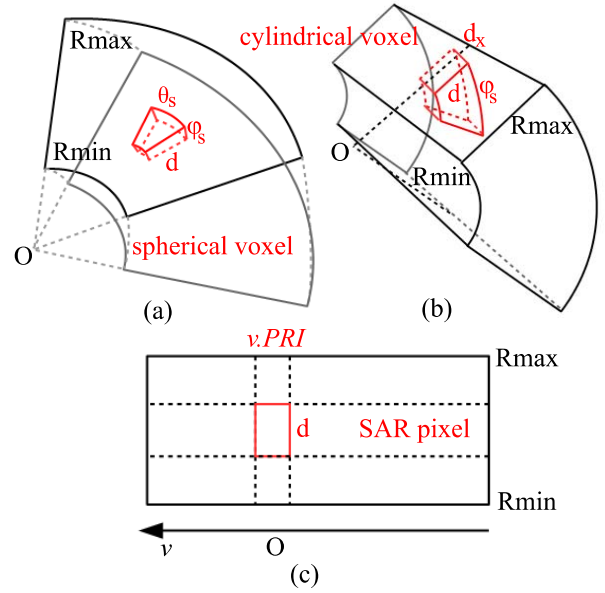


Fig. 3. Voxel generated by (a) spherical beam sweeping by a stationary radar, (b) cylindrical beam sweeping performed by a stationary radar, and (c) SAR-type scanning obtained from the uniform linear motion of the radar with constant velocity v . The point O represents the radar position.

Equations (1)–(3) are valid here since the duty-cycle T/PRI of the FMCW radar is low ($T/PRI = 5\%$ for $PRI = 100$ ms). The voxel volume for the three solutions considered here is illustrated in Fig. 3.

B. Indoor Sensor Interrogation at 1.3 m and Definition of Statistical Estimators of the Relative Humidity

Wireless measurements are first performed to study the linearity and the full-scale measurement range of the Van-Atta reflectarray humidity sensor. For this purpose the passive sensor is placed in a homemade chamber with a humidity controller and a reference humidity sensor (Fisherbrand 90954) with an accuracy of $\pm 5\%$.

The chamber has a very low relative permittivity (ε_r very close to 1) to minimize electromagnetic reflections. The ambient humidity inside the chamber increases by heating a humid sponge. The relative humidity and the temperature are recorded at the beginning and at the end of each measurement.

For this very first experiment, the distance between the radar and the sensor is set at 1.3 m. The spherical sweeping (solution n°1) is chosen with an angle of $\pm 10^\circ$ in azimuth and $\pm 10^\circ$ in elevation requiring the recording of 441 beat frequency spectra (about 3960 voxels) at different interrogation directions.

The relative humidity can be remotely derived from the calculation of statistical estimators. The estimator can be defined as the echo level of specific voxel or as the combination of echo levels at different voxels.

When defining a statistical estimator of the humidity from the analysis of the 3-D (or 2-D) radar image, four key parameters must be considered: the achievable dynamic range D of the estimator; the sensitivity η of the estimator with respect to humidity; the linearity of the estimator with respect to

humidity (this linearity is characterized by the coefficient of determination R^2); and finally, the standard error or precision ε , that is, the difference between the value of the estimator and the value given by the linear regression of the estimator with respect to humidity.

Three statistical estimators are proposed here to derive the relative humidity from the measured scattering data as follows:

- 1) the value e_{Max} of the—unique—voxel containing the maximal echo level;
- 2) the mean echo level e_A of all voxels values in the total interrogated volume;
- 3) the estimator e_S such that $s = \phi(e_S)$ where s is a given number of voxels and ϕ denotes Gaussian-like distribution of the measured echo level. This function is given by

$$\begin{cases} \varphi(x) = \frac{K}{\sigma} \cdot G\left(\frac{x-\mu}{\sigma\sqrt{2}}\right) \cdot \Phi\left(\alpha \cdot \frac{x-\mu}{\sigma}\right) \\ \text{with } G(x) = \frac{\exp(-x^2)}{\sqrt{2\pi}} \\ \text{and } \Phi(x) = \frac{1}{2} \left(1 + \operatorname{erf}\left(\frac{x}{\sqrt{2}}\right)\right) \end{cases} \quad (4)$$

where K is the scaling factor, μ denotes the shift (in dB) of the distribution, σ designates the standard deviation, and erf is the error function. Compared with our earlier work [4], the probability density function (PDF) has been modified by defining the domain of ϕ in dB scale and by adding the contribution of the function Φ , which generates an asymmetry controlled by the skewness parameter α [11]. This asymmetry allows improving the fitting of the PDF to the measurement results and then deriving a more accurate description of the echo level distribution. Measurement results are fitted to ϕ for given values of the parameters μ , σ , K , and α , followed by a Kolmogorov–Smirnov test [12] between the PDF and the measurement data. The Kolmogorov–Smirnov test can be applied here if the parameters of the distribution are correctly defined. If the resulting two-tailed p-value of the test is lower than 95%, the echo level interval is reduced and ends to a success test with $p \geq 95\%$. The sensitivity of this test is often higher at the center of the distribution where the impacts on the tails of the distribution are limited. For a better sensitivity of this test at the tails of the distribution (i.e., for high echo levels or for noise echo levels), the Anderson–Darling [13] test could be preferred.

To enlighten the physical meaning of the statistical estimator e_S , the distribution ϕ is plotted in Fig. 4 for various relative humidities. It can be observed that the profile of the distribution varies with RH. As RH changes the estimator e_S varies, and depends on the number s of voxels: a small number of voxels (including extrapolating values inferior to 1) leads to high dynamic range D at the expense of low measurement precision ε . The requirement for optimal value of s (if exists) could be a precision from e_S close to one obtained from e_{Max} and a sensitivity of e_S better than one achieved by e_{Max} .

The three estimators e_{Max} , e_A , and e_S are computed for RH varying from 38% to 69% (see Fig. 5). The resulting key above-defined parameters D , η , R^2 , and ε of these estimators

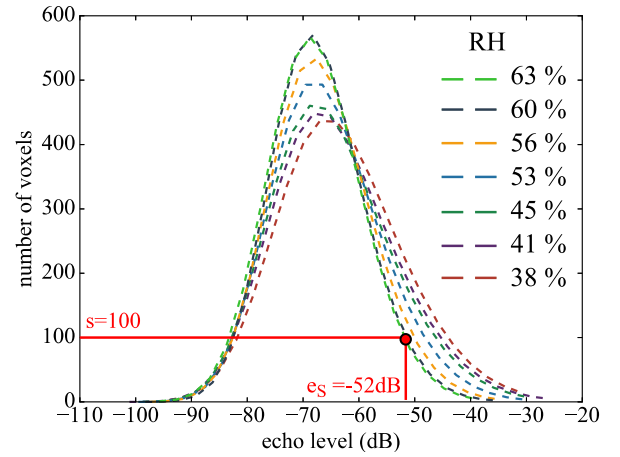


Fig. 4. Measured Gaussian-like distribution of the echo level for various relative humidities using the Van-Atta reflectarray humidity sensor interrogated at 1.3 m. From this statistical distribution, the estimator e_S is computed for a given number of voxels. As indicated in the image, for a relative humidity 63% and $s = 100$ voxels, the estimator e_S is found to be of -52 dB.

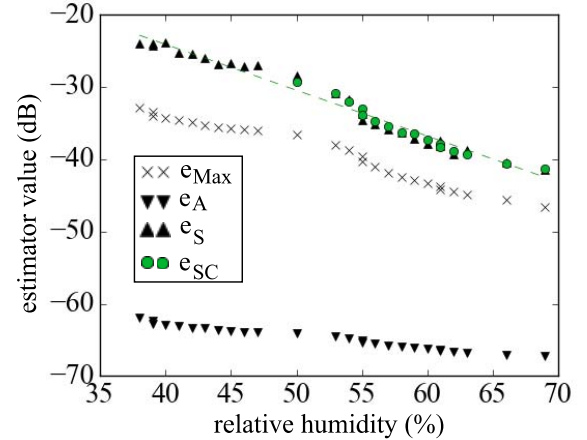


Fig. 5. Statistical estimators e_{Max} , e_A , e_S , and e_{SC} (see text) as a function of relative humidity using the Van-Atta reflectarray humidity sensor interrogated at 1.3 m. A correction (green dots) is applied on the estimator e_S ($s = 4$ voxels) by taking advantage of the linear behavior of the estimator e_A .

are reported in Table I. Here, $s = 4$ voxels which leads to a sensitivity (0.6 dB/%) higher than e_{Max} (0.4 dB/%). In order to improve the precision (ε) and the linearity (R^2) of the estimator e_S , a correction is applied based on the high linearity of the estimator e_A . To apply this correction, let a_A and a_S be the sensitivities with respect to relative humidity RH of estimators e_A and e_S , respectively. Moreover let b_A and b_S the intercepts (estimator value for RH = 0%) of linear regressions of the estimators e_A and e_S , respectively. As a consequence, it can be written that $e_A = a_A \cdot \text{RH} + b_A$ and $e_S = a_S \cdot \text{RH} + b_S$. For $\text{RH} > 50\%$, the correction consists of computing the following estimator:

$$e_{\text{SC}} = \frac{a_S}{a_A} (e_A - b_A) + b_S. \quad (5)$$

From this estimator, the RH is obtained with a better precision (0.7 dB instead of 0.9 dB) and an improved linearity ($R^2 = 0.98$). Consequently, the analysis of statistical estimators like e_S offers many advantages as it allows improving the

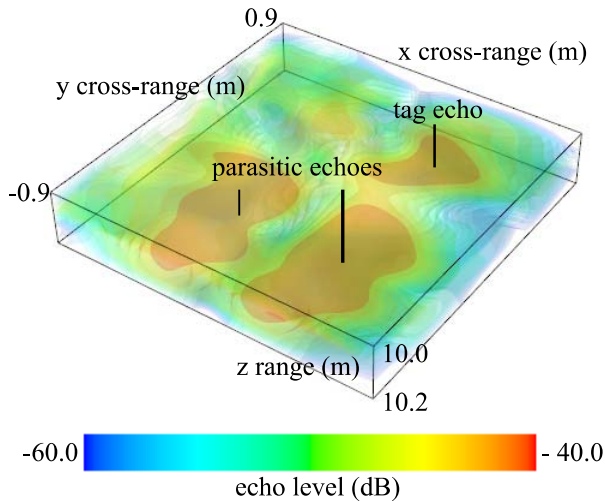


Fig. 6. 3-D echo level of the scene at a range R between 10 and 10.2 m. It includes the echo response of the tag for $RH = 37\%$ as well as parasitic echoes (clutters).

sensitivity of the passive sensor by at least 50% without impacting the measurement precision.

C. Indoor Interrogation at 10 m and Sweeping Combination Method

When performing the spherical beam sweeping with a stationary radar (solution $n^{\circ}1$), the volume of the voxel increases with distance R [see (1)]. From (2), a cylindrical sweeping (solution $n^{\circ}2$) can be used to reduce the voxel volume. However, the challenge is to retrieve the voxel of highest echo when the position of the sensor is not accurately known at long interrogation ranges. For the sake of illustration the Van-Atta reflectarray humidity sensor is placed at 10 m from the radar. A spherical sweeping (solution $n^{\circ}1$) is performed with an angle of $\pm 5^\circ$ in azimuth and $\pm 5^\circ$ in elevation, generating a volume containing 270 voxels. Fig. 6 is the resulting 3-D representation of the ambient echo level at distances (z -direction) between 10 and 10.2 m for $RH = 34\%$. It is displayed with isosurfaces [14] (layers of the same echo level) which are superimposed on a 3-D Cartesian grid. Inside the volume are included the echo levels of interest but also spurious echoes (clutters). If the clutter is not removed, the humidity estimation is erroneously obtained from the estimator called e_{MaxERR} . Nevertheless, the clutter can be ignored by focusing the analysis on echoes of a small volume incorporating the sensor. In this case a second estimator is extracted, called here e_{MaxOPT} . However, this estimation requires knowing the exact position of the sensor (or in another perspective the exact position of the radar). Another solution consists of performing a step-by-step linear translation of the radar (perpendicular to the direction of interrogation) after each spherical sweeping. This method (combination of solutions $n^{\circ}1$ and $n^{\circ}2$) is called here the *sweeping combination* as it is equivalent to combine data from cylindrical and spherical sweepings. From solutions $n^{\circ}1$ and $n^{\circ}2$ and the resulting PDF defined in (4), the new statistical estimator $e_S(n)$ is computed, where n designates the number of linear steps ($n = 0$ corresponds to solution $n^{\circ}1$). For illustration purpose, five spherical sweepings separated by

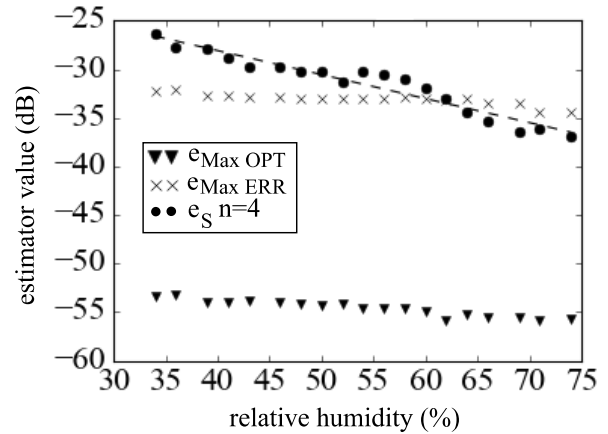


Fig. 7. Statistical estimators e_{MaxOPT} , e_{MaxERR} , and $e_S(n = 4)$ (see text) as a function of relative humidity using the Van-Atta reflectarray humidity sensor interrogated at 10 m. The estimator $e_S(n = 4)$ computed from the sweeping combination solution $n^{\circ}4$ allows retrieving the sensor echo variation despite the high level of parasitic echoes, embedded in the estimator e_{MaxERR} .

a step d_x of 1 cm are performed. Compared to solution $n^{\circ}1$, 5 times more voxels are registered in each beam direction. Moreover, the second Rx channel is used in order to take into account the echoes of around 2700 voxels.

The statistical estimators e_S (with $s = 4$ voxels), e_{MaxERR} , e_{MaxOPT} , and $e_S(n = 4)$ are displayed in Fig. 7 for a relative humidity varying from 34% to 74%. As expected, e_{MaxERR} is biased by spurious echoes which have a constant echo level around -33 dB. If the sensor position is known, e_{MaxOPT} offers good performances with high linearity ($R^2 = 0.97$) and a full-scale dynamic range of 9.5 dB. If the sensor position is unknown, undesirable effects of clutters are attenuated as shown by $e_S(n = 4)$ performances. The sensor echo variation is retrieved with a good linearity ($R^2 = 0.93$) and a precision ε of 1.5%. These results are of course degraded in comparison with ones obtained from the estimator e_{MaxOPT} . However, the fact that the sensor echo level variation is detectable among higher echo levels is remarkable. The impact of the number of steps adopted in solutions $n^{\circ}1$ and $n^{\circ}2$ (sweeping combination) can be observed in Table I. As expected, for the solution $n^{\circ}1$ only (spherical sweeping) the relative humidity estimation is not as good as for the combined solutions with $n \geq 1$ ($R^2 = 0.88$ and $\varepsilon = 5\%$). This is due to a less number of voxels and informative echo data in solution $n^{\circ}1$ only compared to solutions $n^{\circ}1$ and $n^{\circ}2$ combined.

D. Remote Reading of Humidity Sensor at 2.1 m Using a SAR Beam Scanning

For this experiment, the Van-Atta reflectarray humidity sensor is placed on a conveyor belt at a distance of 2.1 m from the radar. The passive sensor has a constant speed $v = 3.8 \text{ cm}\cdot\text{s}^{-1}$, and the radar system is stationary, as depicted in Fig. 8(a). This configuration is equivalent to solution $n^{\circ}3$ (SAR scanning) introduced in Section II-A in which the humidity sensor is stationary and is interrogated by a radar having a uniform linear motion with constant velocity of $v = 3.8 \text{ cm}\cdot\text{s}^{-1}$.

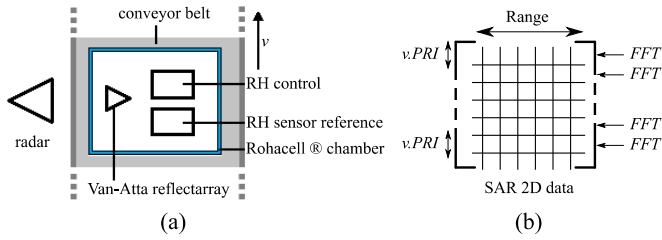


Fig. 8. (a) Van-Atta reflectarray humidity sensor placed on a conveyor belt at a distance and interrogated by a stationary radar. An equivalent configuration would consist of interrogating a stationary sensor by a radar having a uniform linear motion with constant velocity. The passive humidity sensor is located at 2.1 m from the radar, and the conveyor speed is of $3.8 \text{ cm}\cdot\text{s}^{-1}$. (b) Generated 2-D SAR data grid.

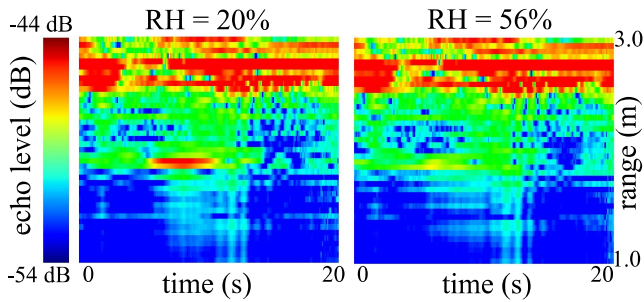


Fig. 9. 2-D display of the electromagnetic echo of Van-Atta reflectarray humidity sensor echo located at 2.1 m in front of the radar, for RH = 20% (left) and RH = 56% (right). High echoes observed at 3 m are due to surrounding clutters.

The pulse repetition interval PRI of the radar is of 100 ms and leads to a duty-cycle T/PRI of 5%. From the radar and antenna parameters, the stop-and-go approximation can be used and Doppler shift effects can be neglected [15]. The 2-D radar data grid is then generated by applying an FFT on the time signal at each PRI [Fig. 8(b)]. 2-D radar images for different values of relative humidity are displayed in Fig. 9. In Fig. 9, the ordinate is the interrogation range (theoretical resolution d of 7.5 cm) while the abscissa is the cross-range (resolution d_x of 3.8 cm with a PRI of 100 ms). The echo levels at distances close to 2.1 m are mainly due to the sensor backscattering and depend on the relative humidity. For RH = 20% the sensor backscattering is maximal and is associated with the highest echo level. For RH = 56%, the resonant frequency of the reflectarray is found to be out of the frequency band of the radar. Consequently a low echo level is measured. Additional high echoes can be observed at 3 m and are the constant clutters from the environment. These undesirable echoes must not be taken into account in the estimation of the relative humidity. From (3), the surface resolution S_{SAR} is here of 28.5 cm^2 . This resolution depends on speed v of the sensor when using stationary radar (or of the radar velocity when interrogating stationary sensor) and on the PRI. The estimator e_{Max} is reported in Table I for different values of PRI. It has been calculated for a relative humidity varying from 20% to 56%. A good linearity ($R^2 = 0.99$) and precision (1 dB) of e_{Max} is obtained with a dynamic range of 9 dB. As expected, both the linearity and precision are

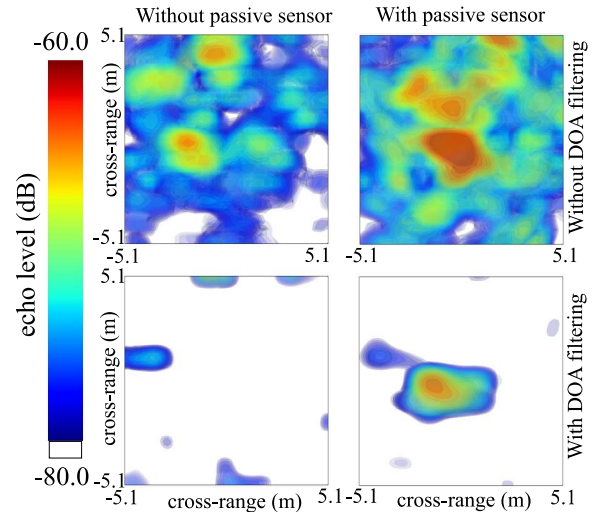


Fig. 10. 2-D echo level of the scene at a range R between 57.5 and 58.5 m with (right) and without (left) the passive humidity sensor. A picture of the experimental setup is shown in Fig. 2(b). Due to the cross-polarization effect, the sensor is detectable at these long distances. A DoA filter (bottom) removes the undesirable echoes (clutter) and the multipath generated by the walls of corridor.

degraded when the PRI exceeds 1 s.

From all the results reported in Table I, it can be observed that the estimators performance depend on the reading range: more the tag is close to the radar more the sensitivity is raised. (The sensitivity reaches 0.6 dB/% at 1.3 m.) This is due to a degradation of the SNR as the reading range increases. Nevertheless, the relative humidity can be derived from a calibration process and link budget. Independently of the interrogation range, the accuracy of the proposed estimators can be improved. For the sweeping combination (solutions $n^{\circ}1$ and $n^{\circ}2$), the linearity (R^2) increased with the number of translations ($n = 4$). Moreover, for the SAR beam scanning (solution $n^{\circ}3$), the sensitivity and linearity are enhanced from reducing the PRI of the radar (or equivalently, from generating finer radar data grids).

E. Long-Range Radar Interrogation (58 m) of the Passive Humidity Sensor and DoA Analysis

The Van-Atta humidity sensor reflectarray is now located at 58 meters from the radar and for a relative humidity of 48%. A picture of the experimental setup is shown in Fig. 2(b). Due to hardware limitations, only $N = 1024$ samples are used here for discretizing the chirp up-ramp frequency modulation. As a consequence, it is no more possible at this distance to perform echoes measurement with the radar bandwidth of 2 GHz. The bandwidth can be set to 1.2 GHz leading to a lower theoretical depth resolution ($d = 12$ and 5 cm) and a theoretical maximal interrogation range of $d \times N/2 = 64$ m. Moreover, the x -range and y -range resolutions are found to be of 1 m for the adopted 1° mechanical sweep step. Fig. 10 displays the 3-D representation of the ambient echo (clutter) level at distances (z -direction) between 57.5 and 58.5 m. The estimator e_{Max} (that is, the value of highest echo magnitude in the volume of analysis) for the passive sensor echo levels

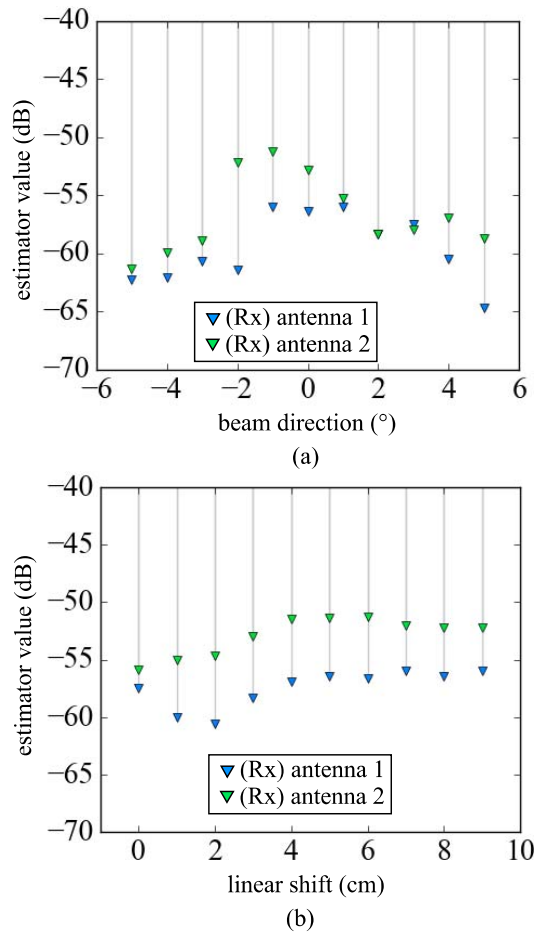


Fig. 11. Humidity estimator e_{Max} computed from the measured electromagnetic echoes of a passive sensor located at 58 m from the radar as a function of (a) different beam directions with a cylindrical sweeping (solution n^o2) and (b) different cross-range positions with a spherical sweeping (solution n^o1). The backscattered signal is received by two antenna arrays (antenna 1 and antenna 2) of 1×5 patch antennas separated by a distance of 6 mm with the gain of 8.6 dBi and the beamwidth of 60° and 25° in azimuth and elevation, respectively.

over the isosurfaces found to be of -56.2 dB. The Van-Atta reflectarray humidity sensor is visible among the clutter with a dynamic range difference of 6 dB, knowing that the maximal echo from the clutter is $e_{\text{Max}} = -62.1$ dB. This difference of 6 dB has been measured by analyzing e_{Max} with and without the reflectarray. Despite the lower depth and cross-range resolutions, it is very encouraging to observe that the echo level of the clutter is very small compared with the echo of the humidity sensor at such long distances. If the sensitivity of 0.2 dB/% is preserved, the full-scale dynamic range (which is the echo level difference between the highest and lowest echo levels generated by the reflectarray) is close to 9 dB. This long-range indoor interrogation is possible by using the cross-polarization effect of the reflectarray: the depolarization effect becomes a discriminant criterion because it was observed that the environment depolarizes significantly less than the passive sensor.

To illustrate the impact of the radar position and of the corridor on the long-range remote derivation of the relative humidity, the estimator e_{Max} is now calculated for different beam

directions and different linear shifts by performing a sweeping combination (solutions n^o1 and n^o2). The electromagnetic signals backscattered by the sensor are received (Rx) by two antenna arrays (Antenna 1 and Antenna 2) of 1×5 patch antennas separated by a distance of 6 mm with the gain of 8.6 dBi and the beamwidth of 60° and 25° in azimuth and elevation, respectively. Results are shown in Fig. 11 for the two antennas arrays. It can be observed that the echo level difference between the two reception channels at the same position is of 10 dB in Fig. 11(a). These differences may originate in the retrodirective effect of the Van-Atta reflectarray, which reflects the signal at a specific angle. Since the DoA is not equal to 0°, a difference of echo levels occurs. It enlightens the fact that, for long interrogation range of sensor in environments such like corridors, the beam direction of the transmitting antenna has to be controlled with high accuracy ($<1^\circ$) for appropriately interrogating Van-Atta reflectarray sensors. This angle-dependent critical issue can be avoided from performing a beam scanning. Moreover, there is an echo level difference up to 10 dB between two different positions for the common reception channel in Fig. 11(b). It means that the corridor generates multipath propagation and a nonzero azimuthal DoA. The DoA analysis can discriminate the passive sensor echo from undesirable echoes from the clutter. The standard 2-D MUSIC algorithm [16] is used here. The algorithm (not detailed here) assigns a DoA value to each voxel of the radar data grid. A spatial filter is applied to reduce the voxels contribution for which the DoA is higher than -5° . Results are shown in the bottom of Fig. 10. Only the echoes generated by the Van-Atta reflectarray humidity sensor emerge from the 2-D display and the clutter is no more apparent. The DoA analysis is consequently an efficient tool for removing the unwanted echoes (clutter) when interrogating passive sensors at long distance.

IV. CONCLUSION

This paper has reported in detail different configurations to interrogate passive sensors with an FMCW radar and to obtain the high linearity and dynamic measurement range. For this purpose, a Van-Atta reflectarray humidity was used as a passive humidity sensor. The analysis of a multidimensional electromagnetic echo response is explored from three types of beam scanning techniques: a spherical sweeping, a cylindrical sweeping, and a SAR-type scanning obtained from the uniform linear motion of the radar with constant velocity. Statistical estimators of the humidity are defined for the remote derivation of relative humidity from radar echoes. For a sufficient number of voxels, the full-scale dynamic range of 17 dB is obtained with a measurement sensitivity of 0.6 dB/%. By using a method called the sweeping combination, it is possible to estimate the relative humidity among high level of parasitic echoes without knowing the exact position of the passive sensor. For industrial applications, the on-fly measurement of moving passive sensors (uniform linear motion of the radar with constant velocity) is demonstrated at a distance of 2.1 m from the stationary radar: a sensitivity of 0.3 dB/% is

obtained in this case. Finally, thanks to its cross-polarization effect, the Van-Atta reflectarray humidity sensor is detected at the unprecedented long distance of 58 m for different radar positions in an indoor environment (corridor). It was shown that multipath propagation and clutter impact may be removed from applying the DoA analysis to passive sensors echoes.

The next steps are now to explore the limits of the proposed 3-D active remote sensing technique in terms of resolution, precision, and maximal distance of interrogation, as well as multisensors capabilities.

REFERENCES

- [1] A. J. Wixted, P. Kinnaird, H. Larijani, A. Tait, A. Ahmadiania, and N. Strachan, "Evaluation of LoRa and LoRaWAN for wireless sensor networks," in *Proc. IEEE SENSORS*, Orlando, FL, USA, Oct. 2016, pp. 1–3.
- [2] A. Dongare *et al.*, "OpenChirp: A low-power wide-area networking architecture," in *Proc. IEEE Int. Conf. Pervasive Comput. Commun. Workshops (PerCom Workshops)*, Kona, HI, USA, Mar. 2017, pp. 569–574.
- [3] D. C. Malocha, J. Humphries, J. A. Figueroa, M. Lamothe, and A. Weeks, "915 MHz SAW wireless passive sensor system performance," in *Proc. IEEE Int. Ultrason. Symp. (IUS)*, Tours, France, Sep. 2016, pp. 1–4.
- [4] D. Hotte, R. Siragusa, Y. Duroc, and S. Tedjini, "A concept of pressure sensor based on slotted waveguide antenna array for passive MMID sensor networks," *IEEE Sensors J.*, vol. 16, no. 14, pp. 5583–5587, Jul. 2016.
- [5] D. Henry, J. G. D. Hester, H. Aubert, P. Pons, and M. M. Tentzeris, "Long range wireless interrogation of passive humidity sensors using Van-Atta cross-polarization effect and 3D beam scanning analysis," in *IEEE MTT-S Int. Microw. Symp. Dig.*, Honolulu, HI, USA, Jun. 2017, pp. 816–819.
- [6] D. Henry, H. Aubert, and P. Pons, "3D scanning and sensing technique for the detection and remote reading of a passive temperature sensor," in *IEEE MTT-S Int. Microw. Symp. Dig.*, San Francisco, CA, USA May 2016, pp. 1–4.
- [7] D. Henry, H. Aubert, and P. Pons, "Wireless passive sensors interrogation technique based on a three-dimensional analysis," in *Proc. 46th Eur. Microw. Conf. (EuMC)*, London, U.K., 2016, pp. 49–52.
- [8] J. G. D. Hester and M. M. Tentzeris, "Inkjet-printed Van-Atta reflectarray sensors: A new paradigm for long-range chipless low cost ubiquitous smart skin sensors of the Internet of Things," *IEEE MTT-S Int. Microw. Symp. Dig.*, San Francisco, CA, USA, May 2016, pp. 1–4.
- [9] J. G. D. Hester and M. M. Tentzeris, "Inkjet-printed flexible mm-Wave Van-Atta reflectarrays: A solution for ultralong-range dense multitag and multiresponsive chipless RFID implementations for IoT smart skins," *IEEE Trans. Microw. Theory Techn.*, vol. 64, no. 12, pp. 4763–4773, Dec. 2016.
- [10] B. A. Atayants, V. M. Davydochkin, V. V. Ezerskiy, S. V. Parshin, and S. M. Smolskiy, *Precision FMCW Short-Range Radar for Industrial Applications*. Norwood, MA, USA: Artech House, 2014.
- [11] S. O. Piper, "Receiver frequency resolution for range resolution in homodyne FMCW radar," in *Proc. Conf. Nat. Telesyst. Conf.*, Atlanta, GA, USA, 1993, pp. 169–173.
- [12] A. S. Wahed and M. M. Ali, "The skew-logistic distribution," *J. Stat. Res.*, vol. 35, pp. 71–80, Jan. 2001.
- [13] F. J. Massey, Jr., "The Kolmogorov-Smirnov test for goodness of fit," *J. Amer. Stat. Assoc.*, vol. 46, no. 253, pp. 68–78, 1951.
- [14] M. A. Stephens, "EDF statistics for goodness of fit and some comparisons," *J. Amer. Stat. Assoc.*, vol. 69, no. 347, pp. 730–737, 1974.
- [15] P. Ramachandran and G. Varoquaux, "Mayavi: 3D visualization of scientific data," *Comput. Sci. Eng.*, vol. 13, no. 2, pp. 40–51, Mar./Apr. 2011.
- [16] A. Meta, P. Hoogeboom, and L. P. Ligthart, "Signal processing for FMCW SAR," *IEEE Trans. Geosci. Remote Sens.*, vol. 45, no. 11, pp. 3519–3532, Nov. 2007.
- [17] F. Belfiori, W. van Rossum, and P. Hoogeboom, "Application of 2D MUSIC algorithm to range-azimuth FMCW radar data," in *Proc. 9th Eur. Radar Conf.*, Amsterdam, The Netherlands, 2012, pp. 242–245.



Dominique Henry received the M.S. degree in electrical engineering from INP ENSEEIHT, Toulouse, France, in 2012. He is currently pursuing the Ph.D. degree in collaboration with the Laboratory for the Analysis and Architecture of Systems (LAAS), National Center for Scientific Research (CNRS), Toulouse, and Ovalie Innovation, Auch, France.

From 2013 to 2014, he was a Research Engineer with LAAS-CNRS. His current research interests include the use of microwave radars for agricultural applications, remote sensing of passive sensors, development of radar interrogation techniques and smart antennas in constraint environments, and microwave imaging and signal processing.



Jimmy G. D. Hester received the bachelor's and M.S. degrees in electrical and signal processing engineering (with a major in radio frequency electronics) from INP Toulouse, ENSEEIHT, Toulouse, France, in 2012 and 2014, respectively, and the M.S. degree in electrical and computer engineering from the Georgia Institute of Technology, Atlanta, GA, USA, in 2014, where he is currently pursuing the Ph.D. degree in electrical and computer engineering.

He spent two preparation years in fundamental chemistry, maths, and physics. He is currently a Research Assistant with the ATHENA Group, Georgia Institute of Technology. He has been developing solutions for the use of carbon nanomaterials, as well as optimized RF structures toward the implementation of inkjet-printed flexible low-cost ubiquitous gas sensors for Internet of Things and smart skin applications. He is involved in the entire development process from the development of inkjet inks, improvement of fabrication methods, sensor component design, high-frequency characterization and environmental testing to the design, and simulation and fabrication of the RF system embedding the sensor. His current research interests include interface between radio frequency engineering and material science, in the form of flexible electronics technologies and nanotechnologies.



Hervé Aubert (SM'99) was born in Toulouse, France, in 1966. He received the Eng.Dipl. and Ph.D. degrees (Hons.) in electrical engineering from the Institut National Polytechnique (INPT), Toulouse, in 1989 and 1993, respectively.

In 2006, he joined the Laboratory for the Analysis and Architecture of Systems (LAAS), National Center for Scientific Research (CNRS), Toulouse. Since 2001, he has been a Full Professor with INPT. Since 2015, he has been the Head of the Micro- and Nano-Systems for Wireless Communications

Research Group, LAAS-CNRS.

Dr. Aubert is a member of the URSI Commission B. He has been serving as a Subject Editor for *Electronics Letters* since 2016, an Associate Editor for *Electronics Letters* since 2015, and an Editorial Board member of the *International Journal of Antennas and Propagation* since 2014 and the *International Journal of Microwave Science and Technology* since 2010. He was the General Chairman of the European Microwave Week, Paris, France, in 2015, and a Technical Program Committee member of the following international conferences: the European Microwave Week in 2013, 2014 (Subcommittee Chair of Wireless Sensors Networks), 2015, 2016, and 2017; the IEEE Conference on Radio-Frequency Identification Technologies and Applications in 2014; and the Special Session on Advances in Computational Methods in Electromagnetics, Antenna Design, and Applications in 2013 and 2014, and the Symposium on Antenna Technology and Applied Electromagnetics in 2012. He served as a Meta-Reviewer for the European Conference on Antennas and Propagation, Paris, in 2017. He was the Secretary of the IEEE Antennas and Propagation French Chapter from 2009 to 2013, the Vice-Chairman of that chapter from 2004 to 2009, and the Secretary from 2001 to 2004.



Patrick Pons was born in Toulouse, France, in 1963. He received the master's degree in physics, the master's degree (with a specialization in microelectronics), and the Ph.D. degree in electronics from the University of Toulouse, Toulouse, in 1985, 1986, and 1990, respectively.

Since 1991, he has been a Researcher with the Laboratory of Analysis and Analysis of Systems, National Scientific Research Center, Toulouse. He has been the Advisor or Co-Advisor of 30 Ph.D. students. He has authored or co-authored more than

95 papers in refereed international journals and more than 267 communications in international conferences. He holds three international patents in microsensors and has performed three technological transfers with industrial partners. He was involved in 79 funded projects including 13 as a Coordinator (22 international, 31 national, 12 regional, and 14 industrial). His current research interests include microtechnologies and microsensors.

Dr. Pons was a member of the Steering Committee of Micro Mechanics Europe International Conference from 2009 to 2013. He organized the Eurosensors International Conference in 1994 and was the Chairman of the Micro Mechanics Europe International Conference in 2009. He was a member of several program committees for international conferences (MME, IEEE Sensors, Sensornet, and Eurosensors) and is a Reviewer for international journals (*Sensors and Actuators*, *Journal of Micromechanics and Microengineering*, *Microelectronic Engineering*, and *Microsystem Technology*). He has also been an expert for the French Research Agency (ANR) since 2011.



Manos M. Tentzeris (S'94–M'98–SM'03–F'10) received the Diploma degree (*magna cum laude*) in electrical and computer engineering (ECE) from the National Technical University of Athens, Athens, Greece, and the M.S. and Ph.D. degrees in electrical engineering and computer science from the University of Michigan, Ann Arbor, MI, USA.

He was a Visiting Professor with the Technical University of Munich, Munich, Germany, in 2002, a Visiting Professor with GTRI-Ireland, Athlone, Ireland, in 2009, and a Visiting Professor with the

Laboratory for the Analysis and Architecture of Systems, National Center for Scientific Research, Toulouse, France, in 2010. He is currently a Ken Byers Professor in flexible electronics with the School of Electrical and Computer Engineering, Georgia Institute of Technology, Atlanta, GA, USA. He has authored more than 620 papers in refereed journals and conference proceedings, 5 books, and 25 book chapters. He has helped develop academic programs in 3-D/inkjet-printed RF electronics and modules, flexible electronics, origami and morphing highly integrated/electromagnetics, multilayer

packaging for RF and wireless applications using ceramic and organic flexible materials, paper-based radio-frequency identifications (RFIDs) and sensors, wireless sensors and biosensors, wearable electronics, "Green" electronics, energy harvesting and wireless power transfer, nanotechnology applications in RF, microwave MEM's, SOP-integrated (UWB, multiband, millimeter-wave, and conformal) antennas. He is the Head of the ATHENA Research Group (20 researchers). He has served as the Head of the GT-ECE Electromagnetics Technical Interest Group, the Georgia Electronic Design Center Associate Director of RFID/Sensors Research, and the Georgia Institute of Technology, NSF-Packaging Research Center Associate Director of RF Research and the RF Alliance Leader.

Prof. Tentzeris is a member of the URSI-Commission D, a member of the MTT-15 Committee, an Associate Member of EuMA, a Fellow of the Electromagnetic Academy, and a member of the Technical Chamber of Greece. He was a recipient or co-recipient of the 2015 IET Microwaves, Antennas and Propagation Premium Award, the 2014 Georgia Institute of Technology, ECE Distinguished Faculty Achievement Award, the 2014 IEEE RFID-TA Best Student Paper Award, the 2013 IET Microwaves, Antennas and Propagation Premium Award, the 2012 FiDiPro Award in Finland, the iCMG Architecture Award of Excellence, the 2010 IEEE Antennas and Propagation Society Piergiorgio L. E. Uslenghi Letters Prize Paper Award, the 2011 International Workshop on Structural Health Monitoring Best Student Paper Award, the 2010 Georgia Institute of Technology, Senior Faculty Outstanding Undergraduate Research Mentor Award, the 2009 IEEE TRANSACTIONS ON COMPONENTS AND PACKAGING TECHNOLOGIES Best Paper Award, the 2009 E. T. S. Walton Award from the Irish Science Foundation, the 2007 IEEE AP-S Symposium Best Student Paper Award, the 2007 IEEE MTT-S IMS Third Best Student Paper Award, the 2007 ISAP 2007 Poster Presentation Award, the 2006 IEEE MTT Outstanding Young Engineer Award, the 2006 Asia-Pacific Microwave Conference Award, the 2004 IEEE TRANSACTIONS ON ADVANCED PACKAGING Commendable Paper Award, the 2003 NASA Godfrey "Art" Anzic Collaborative Distinguished Publication Award, the 2003 IBC International Educator of the Year Award, the 2003 IEEE CPMT Outstanding Young Engineer Award, the 2002 International Conference on Microwave and Millimeter-Wave Technology Best Paper Award, Beijing, China, the 2002 Georgia Institute of Technology, ECE Outstanding Junior Faculty Award, the 2001 ACES Conference Best Paper Award, the 2000 NSF CAREER Award, and the 1997 Best Paper Award of the International Hybrid Microelectronics and Packaging Society. He has given more than 100 invited talks to various universities and companies all over the world. He was the TPC Chair of the IEEE MTT-S IMS 2008 Symposium and the Chair of the 2005 IEEE CEM-TD Workshop. He is the Vice-Chair of the RF Technical Committee (TC16) of the IEEE CPMT Society. He is the founder and has served as the Chair of the RFID Technical Committee (TC24) of the IEEE MTT-S and the Secretary/Treasurer for the IEEE C-RFID. He has served as an Associate Editor for the IEEE TRANSACTIONS ON MICROWAVE THEORY AND TECHNIQUES, the IEEE TRANSACTIONS ON ADVANCED PACKAGING, and the *International Journal on Antennas and Propagation*. He served as one of the IEEE MTT-S Distinguished Microwave Lecturers from 2010 to 2012. He is one of the IEEE CRFID Distinguished Lecturers.